# Metal Ion Induced Folding of a de Novo Designed Coiled-Coil Peptide

**Wayne D. Kohn, Cyril M. Kay, Brian D. Sykes, and Robert S. Hodges***

*Contribution from the Department of Biochemistry and the Protein Engineering Network of Centres of Excellence, University of Alberta, Edmonton, Alberta, Canada T6G 2H7*

*Received October 23, 1997*

**Abstract:** A disulfide-bridged two-stranded α-helical coiled-coil peptide has been designed which undergoes a random coil to α-helical transition at pH 7 and 20 °C upon metal binding to two sites engineered into the molecule. The metal binding coiled-coil, dubbed $Gla_2Nx$, is composed of identical 35 residue polypeptide chains based on the "Native" heptad sequence repeat $Q_gV_aG_bA_cL_dQ_eK_f$ and contains a Cys substitution for Val at position 2 to allow formation of an interchain disulfide bridge. The coiled-coil structure is destabilized in the apo form by two interhelical i to i′ + 5 ionic repulsions between negatively charged γ-carboxyglutamic acid (Gla) side chains at position 15 of one strand and position 20 of the other strand. In contrast, the folded form is stabilized by metal binding because the metal is chelated by the Gla side chains which otherwise (in the absence of metal) repel one another. One such metal binding interaction was predicted to occur between each pair of repelling Gla side chains. Metal titration monitored indirectly by circular dichroism spectroscopy showed that folding (increased helicity) is directly correlated with addition of 2 equiv of metal ion, supporting the presence of two specific metal-binding sites. The estimated metal dissociation constant, $K_d$, is 0.6 ± 0.3 μM for $La^{3+}$ and 0.4 ± 0.2 μM for $Yb^{3+}$. In addition, $Zn^{2+}$ bound with a $K_d$ of 1.7 ± 0.3 μM but $Ca^{2+}$ had a very weak affinity with a $K_d$ of 18 ± 2 mM. Because folding was associated with a 2:1 ratio of metal to peptide monomer (disulfide-bridged two-stranded coiled-coil), the data suggests cooperativity occurs, so that binding of the second metal is significantly tighter than that of the first, and the measured affinity corresponds to that of the first bound metal. Metal titration monitored by nuclear magnetic resonance spectroscopy also supported the prediction that the peptide binds two metal ions specifically and the conclusion that binding is cooperative because it showed no evidence for the existence of a singly bound intermediate. In addition, $Gla_2Nx$ displays a sharp folding transition over the range from pH 6.2 to 5.2 apparently as a result of Gla side chain carboxylate protonation.

De novo protein design is a relatively new field of research, which is ultimately aimed at the development of novel proteins with useful functional properties. However, this goal has been elusive due to the difficulty in determining the relationship between the primary sequence, three-dimensional structure, and function of a protein. Thus, de novo protein design has been carried out primarily via the so-called minimalistic approach,[1−4] from which it is hoped that a greater understanding of protein sequence−structure relationships may result. Minimalistic de novo designs generally contain only one type of secondary structure, which is most commonly α-helix.[2,3,5,6]

The de novo design efforts of our laboratory have focused on the α-helical coiled-coil motif.[7−9] A coiled-coil consists of two, three, or four amphipathic α-helixes, which contain a heptad sequence repeat denoted by the letters abcdefg. Hydrophobic residues at the a and d positions form a narrow hydrophobic face on each helix, which drives coiled-coil formation through its burial in the subunit interface.[8,10,11] The e and g positions of the heptad repeat flank the hydrophobic face and can participate in interhelical ionic interactions that affect coiled-coil formation and stability.[12−16] These interactions have been shown through structural and stability studies to occur in a specific orientation between position g on one helix and position e′ of the other helix five residues down chain (denoted g−e′ or i to i′ + 5) rather than the alternative e−g′ (i to i′ + 2) interaction, which is blocked by large hydrophobes at position d.[12,17−20] Several recent studies have illustrated the role of

* To whom all correspondence should be addressed. Mailing address: Department of Biochemistry and the Protein Engineering Network of Centres of Excellence, University of Alberta, Edmonton, Alberta T6G 2H7.

(1) DeGrado, W. F.; Wasserman, Z. R.; Lear, J. D. *Science* **1989**, *243*, 622−628.
(2) Bryson, J. W.; Betz, S. F.; Lu, H. S.; Suich, D. J.; Zhou, H. X.; O'Neil, K. T.; DeGrado, W. F. *Science* **1995**, *270*, 935−941.
(3) Betz, S. F.; Bryson, J. W.; DeGrado, W. F. *Curr. Opin. Struct. Biol.* **1995**, *5*, 457−463.
(4) Williams, R. J. P. *Curr. Biol.* **1994**, *4*, 942−944.
(5) Hodges, R. S.; Saund, A. K.; Chong, P. C. S.; St.-Pierre, S. A.; Reid, R. E. *J. Biol. Chem.* **1981**, *256*, 1214−1224.
(6) Talbot, J. A.; Hodges, R. S. *Acc. Chem. Res.* **1982**, *15*, 224−230.
(7) Adamson, J. G.; Zhou, N. E.; Hodges, R. S. *Curr. Opin. Biotechnol.* **1993**, *4*, 428−437.
(8) Hodges, R. S. *Curr. Biol.* **1992**, *2*, 122−124.
(9) Hodges, R. S. *Biochem. Cell Biol.* **1996**, *74*, 133−154.
(10) Hu, J. C.; O'Shea, E. K.; Kim, P. S.; Sauer, R. T. *Science* **1990**, *250*, 1400−1403.
(11) Cohen, C.; Parry, D. A. D. *Proteins: Struct., Funct., Genet.* **1990**, *7*, 1−15.
(12) Kohn, W. D.; Kay, C. M.; Hodges, R. S. *Protein Sci.* **1995**, *4*, 237−250.
(13) Kohn, W. D.; Monera, O. D.; Kay, C. M.; Hodges, R. S. *J. Biol. Chem.* **1995**, *270*, 25495−25506.
(14) Krylov, D.; Mikhailenko, I.; Vinson, C. *EMBO J.* **1994**, *13*, 2849−2861.
(15) Zhou, N. E.; Kay, C. M.; Hodges, R. S. *J. Mol. Biol.* **1994**, *237*, 500−512.
(16) Zhou, N. E.; Kay, C. M.; Hodges, R. S. *Protein Eng.* **1994**, *7*, 1365−1372.

S0002-7863(97)03673-1 CCC: $15.00 
Published on Web 02/03/1998

charged residues at the e and g positions of coiled-coils in directing chain alignment (parallel versus antiparallel)[21,22] and dimerization specificity (heterodimer vs homodimer).[15,23−25]

Design of synthetic peptides or proteins for which large changes in conformation occur upon changes in environment or due to external stimuli such as ligand binding or covalent modification is a major goal in de novo design. For example, peptides which switch from an α-helical to a β-sheet conformation upon a change in pH[26] or redox conditions[27] have been successfully designed. Gonzalez et al. recently designed an α-helical coiled-coil which switches from a dimer to a trimer upon binding of benzene within a cavity in its hydrophobic core.[28] Vinson and co-workers have designed coiled-coils which are stabilized[29] or destabilized[30] by phosphorylation of a serine residue. In coiled-coils, charged residues at the e and g positions can confer environmental sensitivity on stability due to the effects of pH and salt conditions on interhelical ionic interactions. For example a coiled-coil, which is unfolded at neutral pH due to a large number of interhelical repulsions, can be induced to form through a change in pH (resulting in neutralization of repelling side chains) or salt conditions (resulting in charge screening or ion binding).[13,15] Similar effects of salts and pH have been observed for other helix-forming peptides.[31−33]

We have set out to design a coiled-coil peptide which undergoes a metal ion induced folding transition by incorporating a finite number of high-affinity metal-binding sites comprising residues in the e and g heptad positions. The peptide was designed in such a way that ionic repulsions would highly destabilize the coiled-coil and favor the unfolded state. In contrast, in the presence of metal ions, negatively charged side chains which would otherwise repel one another are involved in preferential metal ion binding to the folded structure. The design, structural properties, and metal-binding behavior of the disulfide-bridged two-stranded coiled-coil $Gla_2Nx$ are reported herein.

## Experimental Procedures

**Peptide Synthesis and Purification.** Peptides were synthesized on Rink amide MBHA resin using $N^{\alpha}$-Fmoc (9-fluorenylmethoxycarbonyl) protection strategy and coupling of dicyclohexylcarbodiimide activated hydroxybenzotriazole esters on an Applied Biosystems 430A automated synthesizer.[34] Purification by reversed-phase HPLC[35] was performed at pH 2 and 70 °C on a Synchropak RP-4 C-8 preparative column (21.2 mm i.d. × 250 mm) at 5 mL/min. A two-stage linear AB gradient was used with a 1% B/min rate from 0 to 20% B and a 0.2% B/min rate thereafter. Solvent A was aqueous 0.05% TFA and solvent B was acetonitrile containing 0.05% TFA. Disulfide-bridged peptides were formed from purified reduced peptide by oxidation in a mixture containing 30% DMSO, 67% water, and 3% acetic acid at pH 4, stirred under nitrogen overnight (18−20 h).[36] It was found that the standard air oxidation technique at pH 8 resulted in decarboxylation of Gla residues. Oxidized peptides were repurified under the same conditions as the initial purification with a 2 mL/min flow rate on a Zorbax SB 300 C8 semipreparative column (9.4 mm i.d. × 250 mm) using a two-stage linear AB gradient of 1% B/min from 0 to 15% B and 0.2% B/min thereafter. The final product was characterized by analytical HPLC, amino acid analysis, and electrospray mass spectrometry, as previously described.[12]

**Circular Dichroism Spectroscopy.** Circular dichroism spectroscopy was performed on a Jasco J-500C spectropolarimeter at 20 °C. Urea denaturation, pH titration, and metal titration curves were obtained by monitoring the loss or gain in ellipticity at 222 nm resulting from a change in urea concentration, pH, and metal concentration, respectively. Peptide concentration was determined by amino acid analysis. Lanthanum, ytterbium, and zinc concentrations in stock solutions were determined by EDTA titration using xylenol orange as the end point indicator.[37]

Assuming a two-state coiled-coil to random coil denaturation model, the molar fraction of folded peptide ($f_f$) was calculated from the equation $f_f = ([\theta] - [\theta]_u)/([\theta]_f - [\theta]_u)$, in which $[\theta]$ represents the observed mean residue ellipticity at any particular denaturant concentration and $[\theta]_f$ and $[\theta]_u$ are the mean residue ellipticities of the folded and unfolded states, respectively. The free energy of unfolding ($\Delta G_u$) at each denaturant concentration was calculated from $\Delta G_u = -RT \ln(K_u)$ where $K_u$ is the equilibrium constant of the unfolding process. In the case of the disulfide-bridged peptides, this is simply given by $K_u = f_u/f_f = (1 - f_f)/f_f$. The free energy of unfolding in the absence of denaturant ($\Delta G_u^{H_2O}$) was obtained by linear extrapolation according to the equation $\Delta G_u = \Delta G_u^{H_2O} - m[\text{denaturant}]$.[38] Plots of $\Delta G_u$ vs [denaturant] were made by incorporating only data points near the transition midpoint where the greatest linearity was displayed, and a linear least-squares analysis was performed to obtain the slope term $m$ and $\Delta G_u^{H_2O}$.

Metal titration data were analyzed by least-squares fitting to the equation:

$Y = \{(M_o + P_o + K_d) - [(M_o + P_o + K_d)^2 - 4M_oP_o]^{1/2}\}/2P_o$[37] where $M_o$ is the total metal ion concentration, $P_o$ is the total peptide concentration, and $K_d$ is the metal dissociation constant to be determined. Because $Gla_2Nx$ is assumed to contain two metal binding sites, the value used for $P_o$ in the curve fitting procedure was twice the concentration of the disulfide-bridged two-stranded coiled-coil, which equals the expected total number of binding sites present. The use of this equation assumes that the binding sites in $Gla_2Nx$ behave independently. In this case, $Y$ (fraction folded) $= (\theta_o - \theta_f)/(\theta_s - \theta_f)$ where $\theta_o$ is the molar ellipticity value at 222 nm ($\theta_{222}$) at a particular point in the titration, and $\theta_f$ and $\theta_s$ are the $\theta_{222}$ values of the metal-free and metal-saturated forms of the peptide, respectively.

**Proton NMR Experiments.** Proton NMR experiments were performed on a Varian Unity 300 MHz spectrometer at 24.9 °C with presaturation of the water resonance.[37] Spectrum parameters for the $LaCl_3$ titration were as follows: 256 acquisitions with 8 steady-state

(17) Glover, J. N. M.; Harrison, S. C. *Nature* **1995**, *373*, 257−261.
(18) König, P.; Richmond, T. J. *J. Mol. Biol.* **1993**, *233*, 139−154.
(19) Nilges, M.; Brunger, A. T. *Proteins: Struct., Funct., Genet.* **1993**, *15*, 133−146.
(20) O'Shea, E. K.; Klemm, J. D.; Kim, P. S.; Alber, T. *Science* **1991**, *254*, 539−544.
(21) Monera, O. D.; Zhou, N. E.; Kay, C. M.; Hodges, R. S. *J. Biol. Chem.* **1993**, *268*, 19218−19227.
(22) Monera, O. D.; Kay, C. M.; Hodges, R. S. *Biochemistry* **1994**, *33*, 3862−3871.
(23) Graddis, T. J.; Myszka, D. G.; Chaiken, I. M. *Biochemistry* **1993**, *32*, 12664−12671.
(24) O'Shea, E. K.; Lumb, K. J.; Kim, P. S. *Curr. Biol.* **1993**, *3*, 658−667.
(25) Vinson, C. R.; Hai, T.; Boyd, S. M. *Genes Dev.* **1993**, *7*, 1047−1058.
(26) Mutter, M.; Gassmann, R.; Buttkus, U.; Altmann, K.-H. *Angew. Chem., Int. Ed. Engl.* **1991**, *30*, 1514−1516.
(27) Dado, G. P.; Gellman, S. H. *J. Am. Chem. Soc.* **1993**, *115*, 12609−12610.
(28) Gonzalez, L., Jr.; Plecs, J. J.; Alber, T. *Nature Struct. Biol.* **1996**, *3*, 510−515.
(29) Szilak, L.; Moitra, J.; Vinson, C. *Protein Sci.* **1997**, *6*, 1273−1283.
(30) Szilak, L.; Moitra, J.; Krylov, D.; Vinson, C. *Nature Struct. Biol.* **1997**, *4*, 112−114.
(31) Goto, Y.; Aimoto, S. *J. Mol. Biol.* **1991**, *218*, 387−396.
(32) Goto, Y.; Hagihara, Y. *Biochemistry* **1992**, *31*, 732−738.
(33) Ramalingam, K.; Aimoto, S.; Bello, J. *Biopolymers* **1992**, *32*, 981−992.
(34) Fields, G. B.; Noble, R. L. *Int. J. Peptide Protein Res.* **1990**, *35*, 161−214.
(35) Abbreviations: CD, circular dichroism; NMR, nuclear magnetic resonance; HPLC, high-performance liquid chromatography; $K_d$, dissociation constant; DSS, 2,2-dimethyl-2-silapentane-5-sulfonic acid; MOPS, 3-(*N*-morpholino)propanesulfonic acid; tris, tris(hydroxymethyl)aminomethane; TFE, 2,2,2-trifluoroethanol; TFA, trifluoroacetic acid; i.d., internal diameter; Gla, γ-carboxyglutamic acid; EDTA, ethylenediaminetetraacetic acid.
(36) Tam, J. P.; Wu, C.-R.; Liu, W.; Zhang, J.-W. *J. Am. Chem. Soc.* **1991**, *113*, 6657−6662.
(37) Gariepy, J.; Sykes, B. D.; Hodges, R. S. *Biochemistry* **1983**, *22*, 1765−1772.
(38) Pace, C. N. *Methods Enzymol.* **1986**, *131*, 266−280.

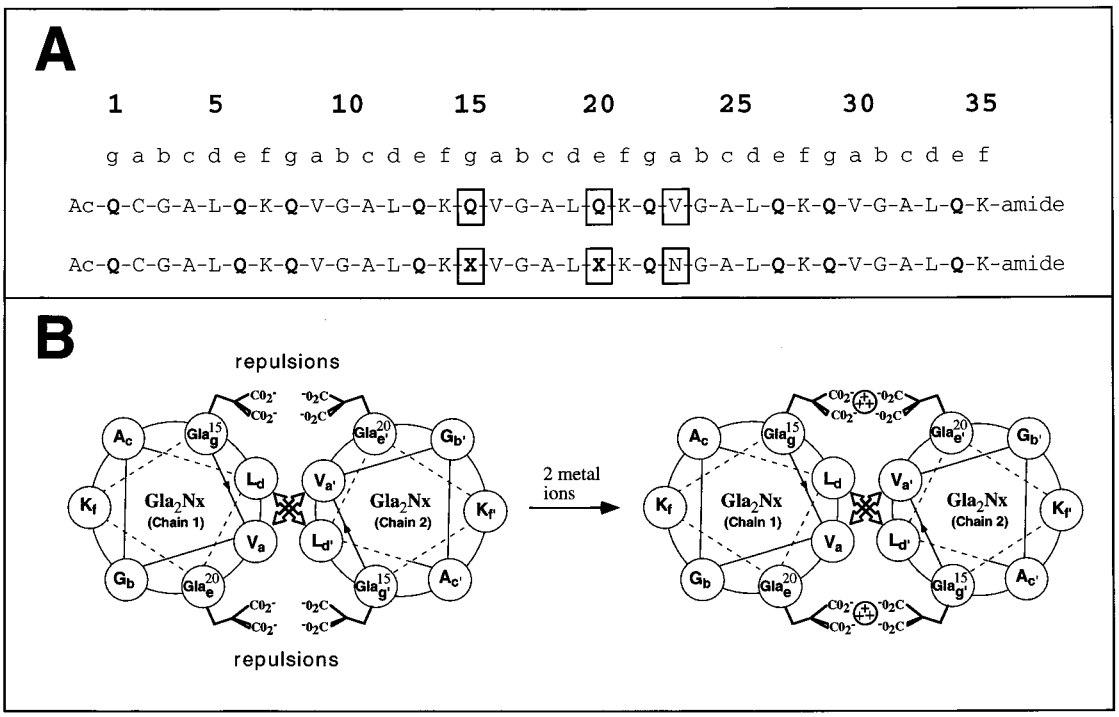


**Figure 1.** (A) Sequences of the "Native" 35-residue model coiled-coil used as a starting point for design of a metal-binding peptide (top) and the metal-binding analogue $Gla_2Nx$ (bottom). A Cys residue at position 2 (heptad position a) allows formation of an interchain disulfide bridge. Substitutions at positions 15, 20, and 23 (shown boxed) are involved in design of $Gla_2Nx$ as described under Peptide Design. In $Gla_2Nx$, the Gla residues are represented by "X". (B) Cross-sectional helical wheel representation of the middle heptad (residues 15−21) of $Gla_2Nx$ in the absence (left) and presence (right) of bound metal ions. The peptide is projected into the page from N- to C-terminus. Interchain a−a′ and d−d′ van der Waals packing interactions occur in the hydrophobic core between Val and Leu residues, respectively, and are indicated with arrows. The Gla side chains at positions g and e flank the hydrophobic interface and can thus lie across the interface and help shield it from water. However, interhelical g−e′ ionic repulsions occur between these negatively charged side chains, greatly destabilizing the coiled-coil structure. Metal ions are proposed to stabilize the folded peptide via chelation of Gla15 on one chain and Gla20′ on the other chain (four carboxylate groups total) to one metal ion. Two such binding sites are present on the coiled-coil, which contains a 2-fold symmetry axis.

preparation scans, sweep width of 4000 Hz, 1.5 s acquisition time with a 2 s delay, pulse width of 7.6 $\mu$s (90°), and spectral line broadening value of 0.5 Hz. The respective values for the $YbCl_3$ titration were: 720 acquisitions with 8 steady-state preparation scans, sweep width of 16 000 Hz, 1.5 s acquisition time with a 2 s delay, pulse width of 7.7 $\mu$s (90°), and spectral line broadening value of 5 Hz. The sample was dissolved in a 50 mM deuterated imidazole, 50 mM KCl buffer at pH 6.9 containing 10% $D_2O$/90% $H_2O$ and 0.1 mM DSS as a chemical shift standard. Peptide concentration was determined by amino acid analysis. Small aliquots of $LaCl_3$ or $YbCl_3$ solution were added to the peptide solution with the total volume changing less than 5% over the titration. The sample was allowed 10−15 min equilibration time after each addition before spectral acquisition.

**Sedimentation Equilibrium Ultracentrifugation.** Sedimentation equilibrium experiments were carried out with a Beckman model E analytical ultracentrifuge equipped with a Rayleigh interference optical system as described previously.[39] Samples were run in a 50 mM tris, 100 mM KCl buffer at pH 6.9. $Gla_2Nx$ at a concentration of about 1 mg/mL (0.13 mM) was run in the absence of lanthanide ion and in the presence of 5 mM $LaCl_3$ (about a 40:1 ratio of metal to peptide). Subsequently, $Gla_2Nx$ at a concentration of about 2 mg/mL (0.26 mM) was run in the presence of 0.25 mM $LaCl_3$ (1:1 ratio) and 2.5 mM $LaCl_3$ (10:1 ratio). A partial specific volume of 0.751 was used, which was obtained from the mass average of the partial specific volumes of the individual amino acids. The data were fit to a single species model using the program Table Curve.

## Results

**Peptide Design.** The metal-binding peptides discussed in this paper are based on the peptide Native-x, which has been used as a control in previous studies of electrostatic effects on coiled-coil stability.[12,13,40,41] Native-x consists of 35-residue peptide chains containing the heptad repeat $Q_gV_aG_bA_cL_dQ_eK_f$ (Figure 1A). Val and Leu residues at positions a and d, respectively, form the hydrophobic face, which packs against the other helix in the dimer interface (Figure 1B). Native-x contains Gln residues at all of the e and g positions, and there are no inter- or intrahelical electrostatic interactions in the peptide, making it a good control for studying electrostatics. A Cys residue substituted for Val at position 2 (heptad position a) allows formation of an interchain disulfide bridge. The disulfide bridge ensures formation of a parallel, in-register coiled-coil and simplifies the folding process from a bimolecular to a unimolecular process. The peptides can also be studied in the absence of a disulfide bridge by treating them with a reducing agent. An "x" after the peptide name indicates the peptide is present in the disulfide bridged form. Native-x forms a stable coiled-coil at 20 °C in pH 7 buffer with a $\Delta G_u$ of about 5.1 kcal/mol.[12]

A successfully designed analogue, which undergoes a metal-induced folding transition, should be unstable enough that it is completely or nearly completely unfolded in the absence of the metal ion. The metal ion must bind to the folded state with a high enough affinity that the free energy of metal binding is enough to overcome the inherent instability of the peptide. Previously, we have shown that $E_2$(15,20)x, which is the same

(39) Zhu, B. Y.; Zhou, N. E.; Kay, C. M.; Hodges, R. S. *Protein Sci.* **1993**, *2*, 383−394.

(40) Kohn, W. D.; Kay, C. M.; Hodges, R. S. *J. Mol. Biol.* **1997**, *267*, 1039−1052.

(41) Kohn, W. K.; Kay, C. M.; Hodges, R. S. *J. Peptide Sci.* **1997**, *3*, 209−223.

as Native-x but with substitutions of Glu for Gln at positions 15 and 20 (positions g and e, respectively, of the middle heptad), is destabilized relative to Native-x by about 1.5 kcal/mol at pH 7. This destabilization is due both to the introduction of interhelical Glu−Glu repulsions and to the lower inherent helical propensity and hydrophobicity characteristics of ionized Glu compared with Gln.[12] Addition of $LaCl_3$ to the buffer increases the stability of $E_2$(15,20)x, likely due to preferential binding of $La^{3+}$ ions to the folded peptide. We have suggested that a metal ion could bridge the Glu residues at positions 15 and 20′, which are otherwise involved in repulsions.[42] However, the binding affinity appears to be weak (on the order of $10^2$ $M^{-1}$).

To amplify the effects of interhelical repulsions and metal-binding on coiled-coil structure, we have employed the unusual amino acid $\gamma$-carboxyglutamic acid (abbreviated Gla), which contains two carboxylate substituents on the $\gamma$-carbon (the side chain is a malonate type group). This amino acid occurs as a posttranslational modification in human blood clotting factors and other proteins, in which it promotes conformational changes by binding $Ca^{2+}$.[43−48] It has previously been shown that lanthanides preferentially bind free Gla at a 1:2 ratio.[49] In such a complex, each Gla side chain can donate two carboxylate ligands so that the metal ion is coordinated by a total of four carboxylate groups. Sperling et al.[49] had suggested that each carboxylate group may interact with the metal ion through both of its oxygen atoms (a bidentate carboxylate−metal interaction). This would fit with the known preference of lanthanides for a higher coordination number by providing a total of eight oxygens from four carboxylates to fill the primary coordination sphere. However, X-ray crystallographic results suggest that interaction of only one oxygen from each carboxylate of a malonate group is the preferred mode of interaction for a variety of metals including lanthanides.[48] We predicted that Gla residues substituted at positions 15 and 20 of each chain of the coiled-coil should result in formation of two lanthanide binding sites (with each site comprising Gla15 of one chain and Gla20′ of the other chain) with much higher affinity than was observed with Glu at those positions (Figure 1B). Destabilization due to Gla−Gla repulsion should also be much higher than for Glu−Glu repulsion due to the extra carboxylate (extra charge) on each side chain.

NMR measurements of the metal−Gla complex gave an approximate distance of 3.7 Å between the $\gamma$-carbon of each Gla group and the metal ion.[49] Computer modeling of $Gla_2Nx$ using the high-resolution X-ray structure of the GCN4 leucine zipper[20] as a template indicated that a metal ion could fit nicely between the Gla15 and Gla20′ side chains. The distance between the $\gamma$-carbons and the metal in this model is about 3.5 Å, in close agreement with the results of Sperling et al.[49] The computer model also predicts that the two bound metal ions are about 11 Å apart and are separated by the hydrophobic core residues (Figure 1B).

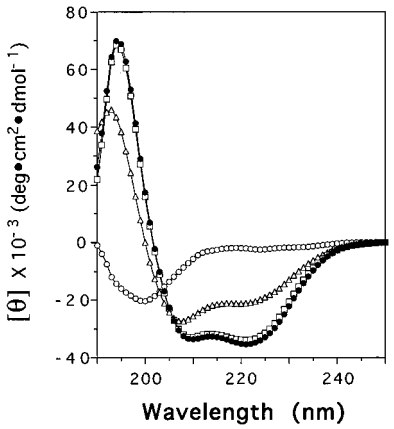


**Figure 2.** Circular dichroism spectra of $Gla_2Nx$ (open symbols) and Native-x (closed symbols). Spectra were collected in a 25 mM MOPs, 25 mM KCl buffer at pH 7 and 20 °C (circles) and also for $Gla_2Nx$ in the same buffer containing 50% TFE (v:v) (triangles) or 5 mM $LaCl_3$ (squares).

We first synthesized the peptide $Gla_2x$, which contains Gln to Gla substitutions at positions 15 and 20. It was found to be about 45% as helical as Native-x by CD spectroscopy at 20 °C in pH 7 buffer (data not shown). Therefore, the coiled-coil was further destabilized by substitution of Asn for Val at position 23 (heptad position a) to obtain the peptide $Gla_2Nx$. Asn occurs frequently at position a in native dimeric coiled-coils and is destabilizing relative to Val but appears to play a role in specifying formation of dimers rather than higher order species due to formation of specific Asn−Asn hydrogen bonds.[50,51]

**Structural Characteristics of $Gla_2Nx$.** The CD spectra of $Gla_2Nx$ and Native-x in benign, pH 7 buffer are shown in Figure 2. The spectrum of Native-x is characteristic of helical structure with minima at 208 and 222 nm and a maximum at 195 nm.[52] The ratio of the molar ellipticities at 222 and 208 nm, $\theta_{222}/\theta_{208}$, is greater than 1, which is indicative of coiled-coil structure.[53] The $\theta_{222}$ value is a measure of the amount of helical content. The $\theta_{222}$ value for Native-x is about −35 000 deg $cm^2$ $dmol^{-1}$, which is approximately the value expected for a fully helical 35-residue peptide.[52] In contrast, $Gla_2Nx$ has a $\theta_{222}$ value of only −2500 and the shape of the CD spectrum is characteristic of a random coil with a minimum at 200 nm.[52] The helix-enhancing solvent TFE substantially increases the $\theta_{222}$ value of $Gla_2Nx$ (Figure 2) to −21 000 (about 60% helical) but has no effect on the helical content of Native-x.[12] Under aqueous conditions and assuming a two-state folding transition, helix formation in $Gla_2Nx$ requires burial of the hydrophobic face through coiled-coil formation, which appears to be inhibited by interhelical Gla−Gla repulsion. In contrast, a 50:50 mixture of TFE and water is able to stabilize an isolated amphipathic helix because of the lower polarity of this solvent mixture and the helix-enhancing properties of TFE.[54,55] The low $\theta_{222}$ of $Gla_2Nx$ in 50% TFE suggests that Gla residues are helix-destabilizing. The $\theta_{222}$ value of $Gla_2Nx$ at 80 °C is about −1600 deg $cm^2$ $dmol^{-1}$. Taking this as the $\theta_{222}$ value of the fully unfolded peptide and the $\theta_{222}$ value of Native-x (−35 000) as the fully

(42) Kohn, W. D.; Kay, C. M.; Hodges, R. S. *J. Peptide Res.* **1997**, in press.
(43) Furie, B.; Furie, B. C. *Cell* **1988**, *53*, 505−518.
(44) Hauschka, P. V.; Carr, S. A. *Biochemistry* **1982**, *21*, 2538−2547.
(45) Prorok, M.; Warder, S. E.; Blandl, T.; Castellino, F. J. *Biochemistry* **1996**, *35*, 16528−16534.
(46) Soriano-Garcia, M.; Padmanabhan, K.; de Vos, A. M.; Tulinsky, A. *Biochemistry* **1992**, *31*, 2554−2566.
(47) Sunnerhagen, M.; Forsen, S.; Hoffren, A.-M.; Drakenberg, T.; Teleman, O.; Stenflo, J. *Nature Struct. Biol.* **1995**, *2*, 504−509.
(48) Zell, A.; Einspahr, H.; Bugg, C. E. *Biochemistry* **1985**, *24*, 533−537.
(49) Sperling, R.; Furie, B. C.; Blumenstein, M.; Keyt, B.; Furie, B. *J. Biol. Chem.* **1978**, *253*, 3898−3906.
(50) Harbury, P. B.; Zhang, T.; Kim, P. S.; Alber, T. *Science* **1993**, *262*, 1401−1407.
(51) Lumb, K. J.; Kim, P. S. *Biochemistry* **1995**, *34*, 8642−8648.
(52) Chen, Y.-H.; Yang, J. T.; Chau, K. H. *Biochemistry* **1974**, *13*, 3350−3359.
(53) Cooper, T. M.; Woody, R. W. *Biopolymers* **1990**, *30*, 657−676.
(54) Lau, S. Y. M.; Taneja, A. K.; Hodges, R. S. *J. Chromatogr.* **1984**, *317*, 129−140.
(55) Sonnichsen, F. D.; Van Eyk, J. E.; Hodges, R. S.; Sykes, B. D. *Biochemistry* **1992**, *31*, 8790−8798.

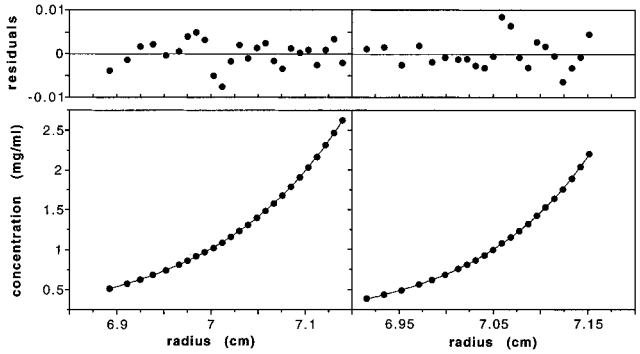


**Figure 3.** Sedimentation equilibrium results for $Gla_2Nx$ at 20 °C and pH 7 in 50 mM tris, 100 mM KCl buffer in the absence (left) and presence (right) of 5 mM $LaCl_3$. Peptide concentration was approximately 1.2 mg/mL (0.16 mM) and 1.0 mg/mL (0.13 mM) in the left and right panels, respectively. A single species (two-stranded monomer) curve fit to the raw data is shown (lower panels) with the residuals from the curve fits (upper panels). The data were collected at a rotor speed of 34 000 rpm.

folded form, indicates that $Gla_2Nx$ is about 3% folded under benign conditions at 20 °C. Addition of $LaCl_3$ to the buffer greatly increases the $\theta_{222}$ value of $Gla_2Nx$ to −34 000 (Figure 2), which is essentially equal to that of Native-x within experimental error. Thus, as predicted, $LaCl_3$ substantially increases the amount of coiled-coil formation by $Gla_2Nx$ at 20 °C from ∼3 to 100%, presumably due to binding of $La^{3+}$ ions to the Gla side chain carboxylate groups.

Sedimentation equilibrium ultracentrifugation experiments were performed on $Gla_2Nx$ at a peptide concentration of ∼1 mg/mL (0.13 mM) both in the presence and absence of 5 mM $LaCl_3$ (about a 40:1 ratio of metal to peptide). The data fit a single-species model for the two-stranded form under both conditions (Figure 3), indicating that no aggregation of this disulfide-bridged two-stranded coiled-coil peptide occurs upon $La^{3+}$ binding. Further evidence against peptide aggregation in the presence of 5 mM $LaCl_3$ comes from the observation that the $\theta_{222}$ value is independent of peptide concentration over the range 10−400 $\mu$M (0.1−3 mg/mL) (data not shown). Additional sedimentation equilibrium experiments were carried out at a peptide concentration of ∼2 mg/mL (0.26 mM) in the presence of either 2.5 mM or 0.25 mM $LaCl_3$ (a 10:1 or 1:1 metal/peptide ratio, respectively). The results were fit to a single-species model equally as well as those shown in Figure 3. Thus, no evidence of aggregation was apparent under any of the conditions tested.

The $^1$H NMR spectrum of $Gla_2Nx$ in the absence of $LaCl_3$ is characteristic of a random coil peptide with little chemical shift dispersion (Figure 4). Saturation of the peptide with $La^{3+}$ causes significant changes in the spectrum. The amount of dispersion is increased, consistent with a more ordered structure. For example, the Leu methyl region at ∼1 ppm shows an increased chemical shift spread. The upfield shift of α-proton resonances is consistent with α-helix formation.[56] In particular, the appearance of a peak at about 3.5 ppm is diagnostic for the α-proton of valine in a helical conformation.[56] A large increase in the number of peaks in the backbone amide region around 7−9 ppm may arise both from greater dispersion and from increased protection from hydrogen exchange [57] as the peptide adopts a helical conformation.

Binding of paramagnetic lanthanide ions leads to perturbations in both the line width (relaxation) and chemical shift of the NMR resonances of a peptide ligand.[58] Both effects are dependent on the distance from the nucleus to the metal ion ($1/r^6$ and $1/r^3$ dependence, respectively) while the chemical shift perturbation is also dependent on the orientation of the nucleus with respect to the metal ion.[58] Typically, some of these shifted resonances appear well outside the envelope of the diamagnetic spectrum. Similarly, a number of highly shifted peaks appear in the $^1$H NMR spectrum of $Gla_2Nx$ in the presence of the paramagnetic lanthanide ytterbium (III), $Yb^{3+}$ (Figure 5). The shifting of selected resonances in the NMR spectrum of $Gla_2Nx$ in the presence of $Yb^{3+}$ is evidence for the binding of the metal ion to specific sites on the peptide. Lanthanide-induced chemical shift and relaxation perturbations can be used to give fairly high definition structural information by fitting of the observed spectrum to a proposed structure.[58,59] Such investigations are currently underway on the $Yb^{3+}$·$Gla_2Nx$ complex.

**pH Dependence.** The helicity of $Gla_2Nx$, as indicated by CD spectroscopy, is highly dependent on pH. As the pH is decreased, side chain protonation reduces interhelical Gla−Gla repulsions and allows increased coiled-coil formation (Figure 6). A similar effect has been observed previously for coiled-coil peptides prevented from folding at neutral pH by interhelical Glu−Glu repulsions.[13,15,23,24] The folding transition takes place over approximately one pH unit from pH 6.2 to 5.2 with the transition midpoint at about pH 5.7. The two $\gamma$-carboxylate groups of free Gla have p$K_a$ values of approximately 5 and 3,[49,60,61] so at pH 7 both should be fully ionized. The observed pH-dependent folding transition of $Gla_2Nx$ may correlate with protonation of one carboxylate per Gla residue. This would leave one negative charge per Gla residue and might be expected to allow complete coiled-coil formation since the analogue $E_2$-(15,20)x is fully folded at pH 7 despite two interhelical Glu−Glu repulsions.[12] It is worth noting that the midpoint of the transition does not equal the p$K_a$ of the carboxylate groups being titrated. This p$K_a$ must be different in the folded and unfolded states in order for the side chain to have an effect on stability.[62] Instead, the p$K_a$ of the carboxylate groups changes from one value, which corresponds to the beginning of the transition, to another value, which corresponds to the end of the transition.[62] Thus, if the transition observed in Figure 6 is indeed due to the protonation of one carboxylate on each Gla side chain, the p$K_a$ would be about 5.2 in the unfolded peptide (comparable to the p$K_a$ in free Gla) and 6.2 in the folded peptide.

**Stability.** As mentioned above, the control Native-x has a $\Delta G_u$ at 20 °C of about 5.1 kcal/mol. Native-x has a urea denaturation midpoint (denoted $[urea]_{1/2}$) of 6.0 M at 20 °C and pH 7 and is unaffected by the addition of a small concentration of $LaCl_3$ (≤50 mM) to the buffer (Figure 7). $Gla_2Nx$ is only about 3% folded at pH 7 and 20 °C (Figure 2), which corresponds to a $\Delta G_u$ of about −2.0 kcal/mol. In the presence of 5 mM $LaCl_3$, it is fully folded (Figure 2), and urea denaturation yields a $[urea]_{1/2}$ value of 3.7 M and a $\Delta G_u$ of 3.1 kcal/mol (Figure 7). At 0.5 mM $LaCl_3$, a $[urea]_{1/2}$ of 3.5 M and $\Delta G_u$ of 2.9 kcal/mol were obtained. The small effect of a 10-fold increase in total $LaCl_3$ concentration on stability is an indication that metal binding is tight. Thus, $Gla_2Nx$ can be

(56) Wishart, D. S.; Sykes, B. D.; Richards, F. M. *J. Mol. Biol.* **1991**, *222*, 311−333.
(57) Englander, S. W.; Mayne, L. *Annu. Rev. Biophys. Biomol. Struct.* **1992**, *21*, 243−265.
(58) Geraldes, C. F. G. C. *Methods Enzymol.* **1993**, *227*, 43−78.
(59) Lee, L.; Sykes, B. D. *Biophys. J.* **1980**, *32*, 193-210.
(60) Marki, W.; Oppliger, M.; Thanei, P.; Schwyzer, R. *Helv. Chim. Acta* **1977**, *60*, 798−806.
(61) Marki, W.; Oppliger, M.; Schwyzer, R. *Helv. Chim. Acta* **1977**, *60*, 807−815.
(62) Yang, A.-S.; Honig, B. *J. Mol. Biol.* **1993**, *231*, 459−474.

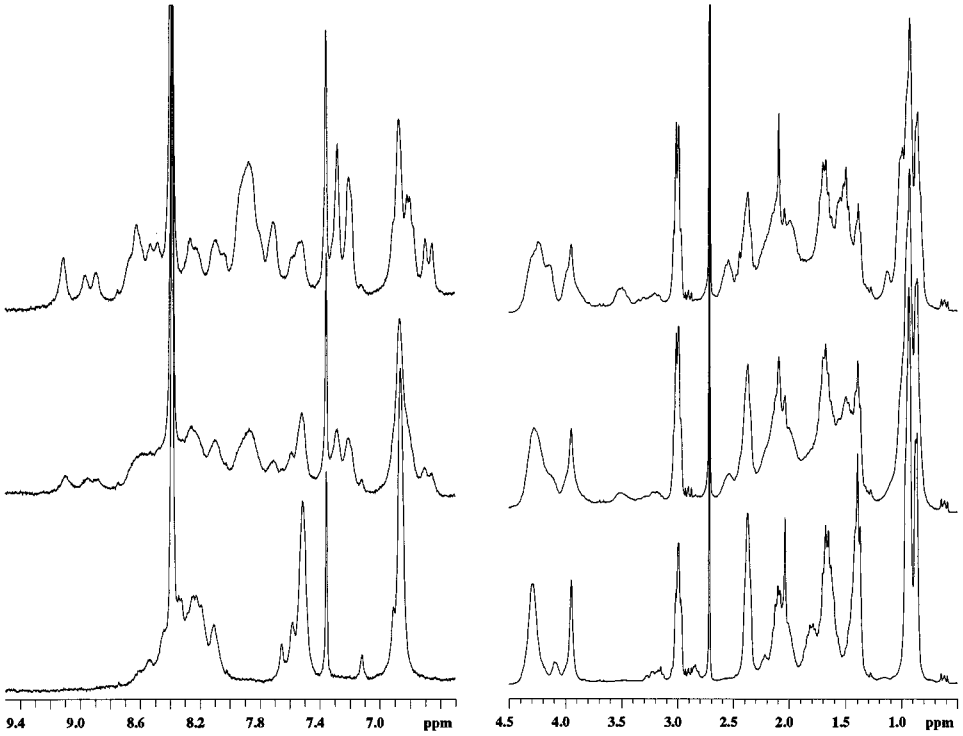


**Figure 4.** One-dimensional 300 MHz $^1$H NMR spectra of $Gla_2Nx$ in the absence of $LaCl_3$ (bottom), presence of 0.5 mM $LaCl_3$ (middle), and presence of 1.0 mM $LaCl_3$ (top) in 50 mM deuterated imidazole, 50 mM KCl, 0.1 mM DSS buffer at pH 6.9 and 25 °C. Peptide concentration was 0.5 mM.

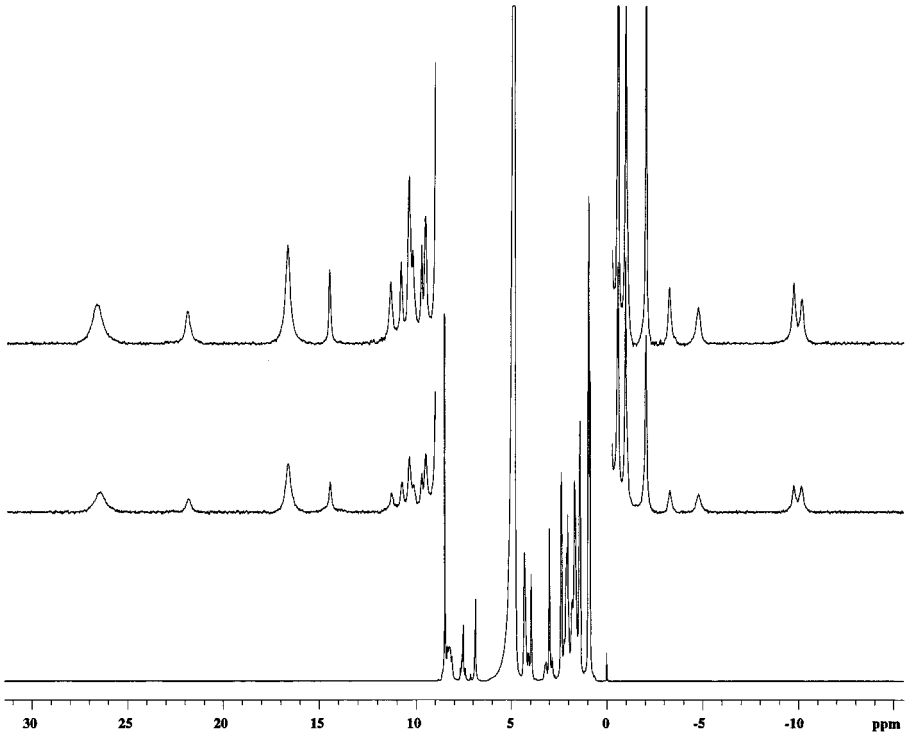


**Figure 5.** One-dimensional 300 MHz $^1$H NMR spectra of $Gla_2Nx$ in the absence of $YbCl_3$ (bottom), presence of 0.6 mM $YbCl_3$ (middle), and presence of 1.2 mM $LaCl_3$ (top) in 50 mM deuterated imidazole, 50 mM KCl, 0.1 mM DSS buffer at pH 6.9 and 25 °C. Peptide concentration was 0.6 mM. The vertical scale in the top and middle spectra is expanded approximately 1000-fold relative to the bottom spectrum.

stabilized by as much as 5.1 kcal/mol by $La^{3+}$ ion binding. In contrast, $E_2(15,20)x$, in which Glu rather than Gla side chains are involved in $La^{3+}$ complexation, was stabilized only 1.1 kcal/mol by 50 mM $LaCl_3$ and 0.2 kcal/mol by 5 mM $LaCl_3$.[42] Therefore, the effect of metal binding on stability is significantly higher in $Gla_2Nx$ because of the chelate effect of the Gla side chain and resulting higher binding affinity.

**Metal Ion Titration Monitored by CD Spectroscopy.** CD spectroscopy can be used to indirectly monitor the binding of a ligand to a protein by measuring the induction of secondary structure upon ligand binding. For $Gla_2Nx$, the induction of helicity can be observed as a function of $LaCl_3$ concentration. Titration of $Gla_2Nx$ with $LaCl_3$ leads to a somewhat linear increase in $\theta_{222}$ with increased $La^{3+}$ concentration (Figure 8A).

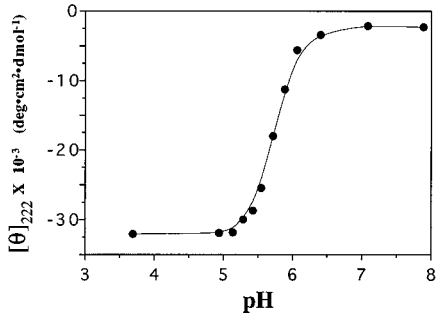


**Figure 6.** Effect of pH on the molar ellipticity at 222 nm ($\theta_{222}$) of $Gla_2Nx$. Data were collected at 20 °C in a 50 mM $PO_4$, 100 mM KCl, 1 mM EDTA buffer. Peptide concentration was 59 $\mu$M.

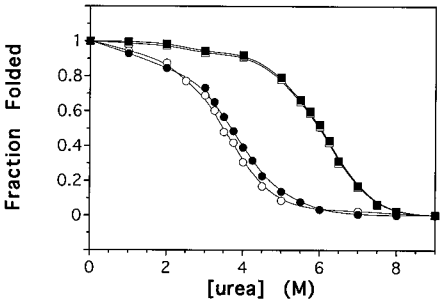


**Figure 7.** Urea denaturation curves for $Gla_2Nx$ (circles) and Native-x (squares) at 20 °C in 50 mM tris, 100 mM KCl, pH 6.9 buffer containing 0.5 mM $LaCl_3$ (open symbols) or 5 mM $LaCl_3$ (closed symbols). The fraction of folded peptide was calculated from the observed mean residue ellipticity at 222 nm as described under Experimental Procedures. Peptide concentrations were in the range 60−70 $\mu$M.

The slope of the titration indicates that, as predicted, the stoichiometry of binding is two $La^{3+}$ ions per peptide. Thus, at the titration midpoint the metal/peptide ratio is about 1:1, and if the straight line is extended to the maximal $\theta_{222}$ value, the metal/peptide ratio is about 2:1. However, the actual amount of $La^{3+}$ required to reach the maximum $\theta_{222}$ value is about 2.5 equiv because the binding is not extremely tight. The data are similar in shape to what is generally obtained for a single binding site and suggests that there is no cooperativity between the sites. However, the actual binding mechanism is not totally clear from these data because it could also be fit to a model with complete positive cooperativity (see Discussion). Fitting of the titration curve to a model of two independent binding sites (see Experimental Procedures) gives an apparent average dissociation constant, $K_d$, of 0.6 ± 0.3 $\mu$M. Titration with $YbCl_3$ yielded a virtually identical result with an apparent $K_d$ of 0.4 ± 0.2 $\mu$M (Figure 8B). Therefore, the smaller radius of $Yb^{3+}$ (0.86 Å) vs that of $La^{3+}$ (1.06 Å) has no effect on binding to $Gla_2Nx$.

Titration with $CaCl_2$ also was found to increase the $\theta_{222}$ value of $Gla_2Nx$ (Figure 8C). However, the maximum $\theta_{222}$ value induced by $Ca^{2+}$ addition is only −21 000 deg cm$^2$ dmol$^{-1}$ (about 60% helix). In addition, the apparent $K_d$ for binding of $Ca^{2+}$ to $Gla_2Nx$ is about 18 ± 2 mM, which is 30 000-fold weaker than the estimated affinity for $La^{3+}$. $Ca^{2+}$ typically has a 100 to 1000-fold lower binding affinity than lanthanides for native proteins such as Gla containing proteins[63,64] and EF hand $Ca^{2+}$ binding proteins,[37,65,66] depending on the lanthanide used and the nature of the binding site. Thus, the metal-binding sites of $Gla_2Nx$ are more discriminatory for lanthanides over $Ca^{2+}$ than those of many native $Ca^{2+}$ binding proteins.

In contrast to the results obtained with $Ca^{2+}$, titration of $Gla_2Nx$ with $ZnCl_2$ illustrated a reasonably high affinity for $Zn^{2+}$ (Figure 8D). In addition, the maximum $\theta_{222}$ obtained from binding of $Zn^{2+}$ was −32 900 deg cm$^2$ dmol$^{-1}$, close to that observed with the two lanthanides. The apparent $K_d$ obtained from the $ZnCl_2$ titration curve is approximately 1.7 ± 0.3 $\mu$M. Thus, $Zn^{2+}$ binds to $Gla_2Nx$ slightly less tightly than either $La^{3+}$ or $Yb^{3+}$, for which the apparent $K_d$ values were about 0.5 $\mu$M. The large difference in the observed $K_d$ values for $Ca^{2+}$ and $Zn^{2+}$ shows that binding affinity is not affected simply by the charge of the metal ion. The smaller radius of $Zn^{2+}$ (about 0.74 Å) vs that of $Ca^{2+}$ (about 1.0 Å) results in a charge density approximately 2.5 times higher, which likely plays a role in the tighter binding of $Zn^{2+}$. However, the differences in the electronic configurations (specifically the presence of 10 electrons in the 3d orbitals of Zn and no electrons in the 3d orbitals of Ca) and preferred coordination numbers, between $Zn^{2+}$ and $Ca^{2+}$ probably also plays a role in their vastly different affinities for binding sites on $Gla_2Nx$.

**Metal Ion Titration Monitored by NMR Spectroscopy.** Binding of lanthanide ions to $Gla_2Nx$ results in new peaks in the $^1$H NMR spectrum arising from the metal-bound, folded form of the peptide (Figures 4 and 5). These peaks gradually grow in intensity at their final chemical shift (the chemical shift observed in the metal-saturated spectrum). Thus, lanthanide binding is in the slow exchange limit on the NMR time scale since no averaging of proton resonances in the bound and unbound states occurs. The slow exchange behavior suggests an upper limit for the $K_d$ of ∼1 $\mu$M, similar to what was estimated by monitoring the titration with CD spectroscopy. The NMR data was not quantitatively analyzed. However, it did provide evidence to support the existence of two binding sites on $Gla_2Nx$ because ∼2 equiv of lanthanide ion led to a maximum in the peak intensity of lanthanide shifted peaks (data not shown). In addition, lanthanide titration leads to the appearance of a single set of lanthanide shifted NMR resonances (presumably due to the final species), which supports the conclusion that metal binding is highly cooperative (see Discussion).

## Discussion

This paper describes the design and characterization of the disulfide-bridged two-stranded coiled-coil peptide $Gla_2Nx$, which undergoes a folding transition upon binding of lanthanide ions to two specific binding sites engineered into the molecule. While this peptide is almost completely unfolded under benign, pH 7 conditions at 20 °C, it becomes highly helical upon addition of a small concentration of lanthanide ion. Indirect measurement of the titration of $Gla_2Nx$ with either $LaCl_3$ or $YbCl_3$ using CD spectroscopy indicates tight binding of two metal ions per coiled-coil with a dissociation constant of around 0.5 $\mu$M. In contrast, $Gla_2Nx$ shows a very weak affinity for $Ca^{2+}$ ($K_d$ ≈ 18 mM), suggesting a dramatic preference for binding trivalent lanthanides over divalent alkali metal ions. $Zn^{2+}$ was found to bind $Gla_2Nx$ with an apparent affinity ($K_d$ ≈ 1.7 $\mu$M) close to that of the lanthanides. Thus, the charge of the metal ion is not the only important factor in controlling the strength of interaction.

The electronic configuration greatly affects the interaction of metal ions with ligands. $Ca^{2+}$, $Yb^{3+}$, and $La^{3+}$ are comparable since all three have no electrons in the ($n$ − 1) d

(63) Furie, B. C.; Mann, K. G.; Furie, B. *J. Biol. Chem.* **1976**, *251*, 3235−3241.
(64) Furie, B. C.; Furie, B. *J. Biol. Chem.* **1975**, *250*, 601−608.
(65) Wang, C.-L. A.; Leavis, P. C.; Horrocks, W. D., Jr.; Gergely, J. *Biochemistry* **1981**, *20*, 2439−2444.
(66) Williams, T. C.; Corson, D. C.; Sykes, B. D. *J. Am. Chem. Soc.* **1984**, *106*, 5698−5702.

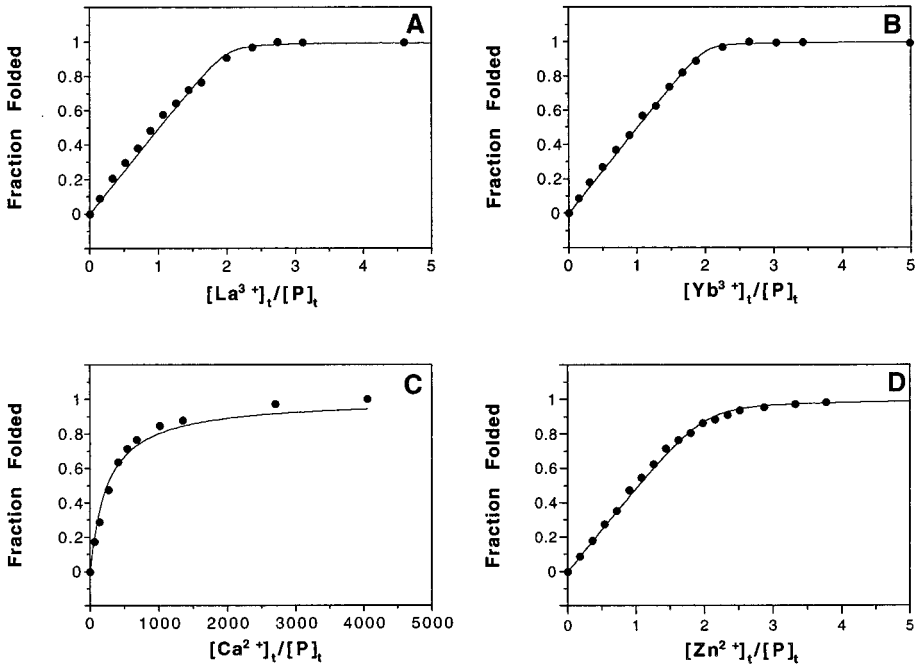


**Figure 8.** Metal titration profiles of $Gla_2Nx$ as monitored by circular dichroism spectroscopy at 20 °C and pH 6.9 in a 10 mM imidazole, 50 mM KCl buffer. The observed mean residue ellipticity at 222 nm was monitored and plotted as the fraction folded (described under Experimental Procedures). Titrations were performed with (A) $LaCl_3$, (B) $YbCl_3$, (C) $CaCl_2$, and (D) $ZnCl_2$. Peptide concentration was 64, 64, 69, and 54 $\mu$M in panels A−D, respectively. The *x* coordinate is the ratio of total metal ion concentration to total peptide concentration. The data were fit using a least squares curve fitting procedure as detailed under Experimental Procedures.

orbitals and are termed as class (a) or "hard" Lewis acids.[67] $Zn^{2+}$ has completely filled 3d orbitals and is considered borderline between classes (a) and (b).[67] The greater the "softness" of the metal ion, the greater the degree to which interactions with ligands can be covalent vs ionic in nature.[67] Accordingly, $Zn^{2+}$ is able to interact with ligands through a higher degree of covalent bond character while the lanthanides and $Ca^{2+}$ tend more toward ionic bonds. Therefore, the higher affinity of $Gla_2Nx$ for the trivalent lanthanides over $Ca^{2+}$ is at least partially due to the higher cation charge allowing for stronger ionic interactions. On the other hand, $Zn^{2+}$ may be able to compensate for a weaker electrostatic interaction with the carboxylate ligands versus that of the trivalent lanthanides due to an increased covalent bond contribution.

Several previous de novo design efforts have focused on enhancement of either α-helical[68−70] or $\beta$-turn[71−73] structure in small peptides through complexation of metal ions. Metal-binding sites have also been incorporated into designed four-helix bundles, resulting in metal ion induced increases in stability but not folding.[74−76] Metal-binding sites engineered into the core of the bundle were found to increase the specificity of the fold by replacing nonspecific hydrophobic interactions with defined metal−side chain interactions.[75] This approach has recently been applied in controlling coiled-coil oligomerization states.[77] Another approach involves incorporation of a metal-binding group at one or both ends of short helix-forming sequences, which allows metal-induced helical bundle assembly.[78−81] The latter studies illustrate metal-induced increases in folding, but the peptides are 30% or more helical in the absence of metal at room temperature. Thus, to our knowledge $Gla_2Nx$ undergoes the largest metal-induced folding transition of a de novo designed peptide. However, while $Gla_2Nx$ was estimated to be stabilized by about 5 kcal/mol from the binding of two $La^{3+}$ ions, the binding of two $Zn^{2+}$ ions to the four-helix bundle H6$\alpha_4$ induced a larger stabilization of 7.8 kcal/mol.[75]

The lanthanide binding affinity of $Gla_2Nx$ is comparable with previous results from Gla-containing peptides and proteins. For example, fragment 12−44 of prothrombin was found to have a single high-affinity ($K_d = 0.55$ $\mu$M) $Gd^{3+}$ binding site, which was postulated to involve two or three Gla residues situated at the ends of a disulfide loop and bridged by a metal ion.[82] Such an interaction is similar to the proposed bridging of Gla15 and Gla20′ of $Gla_2Nx$ by a metal ion. The Gla domains of the blood clotting enzymes Factor X and prothrombin were found to contain two high-affinity sites and a number of lower affinity sites, which bind $Gd^{3+}$ with $K_d$ values of 0.1 to 1 $\mu$M and 10 to 20 mM, respectively.[63, 64] Thus, the affinity of $Gla_2Nx$ for

(67) Pearson, R. G. *J. Am. Chem. Soc.* **1963**, *85*, 3533−3539.
(68) Ghadiri, M. R.; Fernholtz, K. *J. Am. Chem. Soc.* **1990**, *112*, 9633−9635.
(69) Ghadiri, M. R.; Choi, C. *J. Am. Chem. Soc.* **1990**, *112*, 1630−1632.
(70) Ruan, F.; Chen, Y.; Hopkins, P. B. *J. Am. Chem. Soc.* **1990**, *112*, 9403−9404.
(71) Cheng, R. P.; Fisher, S. L.; Imperiali, B. *J. Am. Chem. Soc.* **1996**, *118*, 11349−11356.
(72) Schneider, J. P.; Kelly, J. W. *J. Am. Chem. Soc.* **1995**, *117*, 2533−2546.
(73) Tian, Z.-Q.; Bartlett, P. A. *J. Am. Chem. Soc.* **1996**, *118*, 943−949.
(74) Handel, T.; DeGrado, W. F. *J. Am. Chem. Soc.* **1990**, *112*, 6710−6711.
(75) Handel, T. M.; Williams, S. A.; DeGrado, W. F. *Science* **1993**, *261*, 879−885.
(76) Regan, L.; Clarke, N. D. *Biochemistry* **1990**, *29*, 10878−10883.
(77) Dieckmann, G. R.; McRorie, D. K.; Tierney, D. L.; Utschig, L. M.; Singer, C. P.; O'Halloran, T. V.; Penner-Hahn, J. E.; DeGrado, W. F.; Pecoraro, V. L. *J. Am. Chem. Soc.* **1997**, *119*, 6195−6196.
(78) Ghadiri, M. R.; Soares, C.; Choi, C. *J. Am. Chem. Soc.* **1992**, *114*, 4000−4002.
(79) Ghadiri, M. R.; Soares, C.; Choi, C. *J. Am. Chem. Soc.* **1992**, *114*, 825−831.
(80) Ghadiri, M. R.; Case, M. A. *Angew. Chem., Int. Ed. Engl.* **1993**, *32*, 1594−1597.
(81) Lieberman, M.; Sasaki, T. *J. Am. Chem. Soc.* **1991**, *113*, 1470−1471.
(82) Furie, B. C.; Blumenstein, M.; Furie, B. *J. Biol. Chem.* **1979**, *254*, 12521−12530.

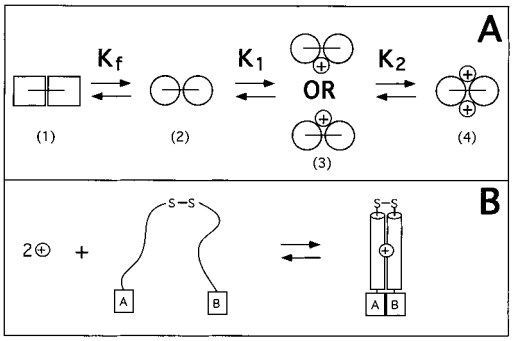


**Figure 9.** (A) Schematic representation of possible species and equilibria involved in lanthanide-induced folding of $Gla_2Nx$, assuming that peptide folding is a two-state process and that the metal ion binds to the folded peptide. Squares stand for unfolded peptide chains and circles represent α-helixes. Four predicted species include the unfolded peptide (1), folded peptide (2), folded peptide bound to one metal ion (3), and folded peptide bound to two metal ions (4). (B) Potential application of metal-induced coiled-coil formation for reversible association of two molecules or domains A and B attached to the C-termini of the disulfide bridged coiled-coil strands. Cylinders represent α-helixes. In both panels, metal ions are represented by a circle with a plus sign.

lanthanide ions is similar to the high affinity sites of intact native Gla domains.

Elucidation of the mechanism for metal binding and resulting induced folding of $Gla_2Nx$ is an interesting problem. A scheme for the process, which assumes two metal binding sites are present in the peptide and that peptide folding is a two-state process, is shown in Figure 9A. In the absence of added metal ion, there is only a small amount of folded peptide (species 2, Figure 9A) present at 20 °C. Added metal ion will preferentially bind to the folded state and remove folded peptide from the unfolded/folded equilibrium, thus shifting that equilibrium toward the folded state. Subsequently, a second metal ion can bind. In curve fitting the CD titration data, we have assumed that the two proposed binding sites are identical and independent ($K_1 = K_2$). Such a situation can occur when the protein is a symmetrical oligomer and each subunit has the same binding site. $Gla_2Nx$ is symmetrical and therefore meets these criteria. Alternatively, if binding of the first ligand changes the structure and enhances binding of subsequent ligands, cooperative binding results. In $Gla_2Nx$, cooperativity could occur as a result of the first bound metal decreasing the flexibility (dynamics) of the folded peptide. Such an effect was suggested to explain the cooperativity observed for $Ca^{2+}$ binding to calbindin despite the absence of a conformational change upon binding of the first $Ca^{2+}$ ion.[83]

In the lanthanide titration of $Gla_2Nx$, monitoring by CD spectroscopy results in a linear increase in helicity with added metal ion. The slope corresponds to a stoichiometry of two metal ions per two-stranded coiled-coil peptide. The data suggest that all the folded peptide being detected by CD is bound to two metal ions. If a significant amount of folded peptide with only one metal bound were present at equilibrium, the CD curve should be steeper and its midpoint should occur at less than a 1:1 ratio of metal ion to two-stranded coiled-coil peptide. Instead, this titration curve suggests that binding of one metal ion stabilizes the "folded" peptide and enhances binding of the second metal ion, such that peptide folding is coincident with binding of two metal ions. Therefore, the data can be interpreted in terms of complete positive cooperativity in which the second binding constant is many orders of magnitude larger than the first. The apparent binding affinity, which was obtained by assuming independent binding sites, would in this case be indicative of the first binding constant only.

The lanthanide titration of $Gla_2Nx$ monitored by NMR also supports the conclusion that metal binding is highly cooperative. Only a single set of lanthanide shifted peaks appear in the NMR spectrum, which it seems must arise from the final structure bound to two metal ions (species 4, Figure 9A). However, if a significant amount of singly bound intermediate (species 3, Figure 9A) were present during the titration, peaks characteristic of that structure would be expected to initially rise and then disappear in the NMR spectrum. Such peaks would originate from protons which are close to and thus perturbed by both metal ions, as observed for the binding of $Yb^{3+}$ to the two $Ca^{2+}$ binding sites of parvalbumin.[59]

There are several potential applications of metal binding peptides. For example, two groups recently designed zinc finger peptides with fluorescent tags, which undergo zinc-dependent fluorescence changes and therefore can act as metal ion sensors.[84,85] Perhaps $Gla_2Nx$ could act as a sensor for lanthanide ions with relatively high specificity over $Ca^{2+}$ ions. More generally, a peptide such as $Gla_2Nx$ could be used for reversible assembly of any two molecules (A and B) covalently attached to the C-termini of the two coiled-coil chains (Figure 9B). In the absence of the metal ion, the coiled-coil would be unfolded and molecules A and B would not be closely associated. Metal-induced folding of the coiled-coil would bring domains A and B together in a well-defined, close proximity and could be used as a switch for some activity that is dependent on A−B association. In addition, because metal ions have catalytic properties, a metal-binding peptide could conceivably be developed into a synthetic enzyme. For example, lanthanides are known to promote phosphate ester hydrolysis and transesterification of RNA,[86] suggesting that a lanthanide-binding peptide could be designed which binds to and cleaves a particular RNA sequence. A metal binding peptide could be used as a carrier for radioimaging metals, specifically technetium-99m or other metals with diagnostic or therapeutic applications.[87] It appears promising that metal-binding peptides will be developed for such uses in coming years.

**Acknowledgment.** We wish to thank Paul Semchuk, Ian Wilson, and Len Daniels for peptide synthesis and purification, Bob Luty for CD spectroscopy, Les Hicks for ultracentrifugation, and Bruce Lix and Linda Golden for NMR spectroscopy. This study was supported by the Protein Engineering Network of Centres of Excellence, Canada. W.D.K. was a recipient of a Natural Sciences and Engineering Research Council of Canada postgraduate scholarship during this project.

JA973673Z

(83) Akke, M.; Forsen, S.; Chazin, W. J. *J. Mol. Biol.* **1991**, *220*, 173−189.

(84) Godwin, H. A.; Berg, J. M. *J. Am. Chem. Soc.* **1996**, *118*, 6514−6515.

(85) Walkup, G. K.; Imperiali, B. *J. Am. Chem. Soc.* **1996**, *118*, 3053−3054.

(86) Morrow, J. R.; Buttrey, L. A.; Shelton, V. M.; Berback, K. A. *J. Am. Chem. Soc.* **1992**, *114*, 1903−1905.

(87) Abrams, M. J.; Murrer, B. A. *Science* **1993**, *261*, 725−730.